RESPONSE OF HELICAL STRUCTURES TO HIGH SPEED PULSES OR WHEN CAN A HELIX BE CALLED AN INDUCTOR?*

Marco S. Di Capua, Nicole E. Molau, and Paul C. Wheeler
Lawrence Livermore National Laboratory
Livermore, California 94550

Abstract

Vacuum and dielectric cored loosely wound helices are widely used in pulse power systems. In one extreme, when the applied pulse length is shorter then the transit time in the helix, helices are used as transit time isolators, to lead signals from high voltage terminals to ground [1]. In the other extreme, for pulse durations that are much longer than the transit time, helices act as conventional inductors and are used for high frequency isolation or as shields for trigger, signal or gas leads to pulse power components. In either case, the use of helices in the presence of fast pulses requires an understanding of their behavior in regimes where time delays associated with wave propagation in the helix are not negligible when compared to the length or risetime of the applied pulse and hence their description as lumped elements is no longer correct. This paper describes the results of analytical approximations, circuit simulations, 3-D time dependent electromagnetic modeling as well as laboratory measurements on helices surrounded by conducting structures. On the basis of these investigations their suitability as voltage measuring devices will be discussed.

Introduction

This paper endeavors to answer two questions regarding the behavior of helical structures in the transient regime. One is: when can a helix be called an inductor? The other one is: can such a helix be used to measure transient voltages in pulse power devices? To answer these questions, we investigate helical structures from theoretical, circuit simulation, 3-D electromagnetic modeling, and experimental viewpoints. We find that the transient behavior of a loosely wound shielded helical structure, in the transient regime, may be described by waves traveling in the wire-above-ground transmission line formed between the helix and the shield. The accuracy of this description is borne by results obtained from circuit simulations, and measurements in the laboratory. The 3-D simulations show that the superposition of the traveling wave fields arising from a linearly rising current equilibrate to the field distributions that would arise from a constant applied voltage. A B-dot probe proximal to the grounded end of the helix superimposes a response to the time derivative of the input voltage and one to the input voltage itself. Waves propagating in the helix yield the first response (current proportional to voltage). The second response (current proportional to the integral of the voltage) arises from the helix behaving as an inductor. Use of the helix for voltage measurements must take into account these two responses.

Theoretical Considerations

Questions arising from the storage of energy in the electric and magnetic fields arising from time varying currents in conductors are deeply rooted in the relationship between electromagnetic and circuit theories [2,3]. Feynman [4] provides a great deal of insight on the subject through a self consistent treatment of the electromagnetic fields within a capacitor and only hints at what the high frequency behavior of an inductor may be. Ollendorf [5] treats in detail the behavior of a parallel wire inductor whose length is no longer negligible compared to the wavelength of electromagnetic radiation. He views an inductor loop as a transmission line of length ℓ_o, inductance per unit length L', capacitance per unit length C'; shorted at $x = \ell_o$. When excited at $x = 0$ by a voltage $V(0,\omega) = V_o e^{j\omega t}$ the impedance at $x = 0$ is:

$$Z(0,\omega) = j(L'/C')^{1/2} \tan\left(\omega \ell_o (L'C')^{1/2}\right) \qquad (1)$$

A series expansion of the tangent for $\omega \ell_o \sqrt{L'C'} \ll 1.0$ yields:

$$Z(0,\omega) = j\omega \ell_o L' \left(1 + \frac{\omega^2}{3} \ell_o^2 L'C' + \ldots\right) \qquad (2)$$

The first term is the "lumped" inductance of the line while the second arises due to the capacitance between the conductors.

Beyond this simple argument, discussions of the winding capacity of inductors have a long and complicated tradition and only a few cases, not applicable to our geometry have been treated successfully. Discussion of the details is beyond the scope of this paper. However, we list some interesting references for the sake of completeness [6,7].

Circuit Model of the Helix

We have investigated the helix whose geometry appears in Fig. 1. The helix consists of five turns of 1 mm-diameter copper wire, with a pitch of 0.5 cm/turn. The helix is 2.5 cm long and has a mean

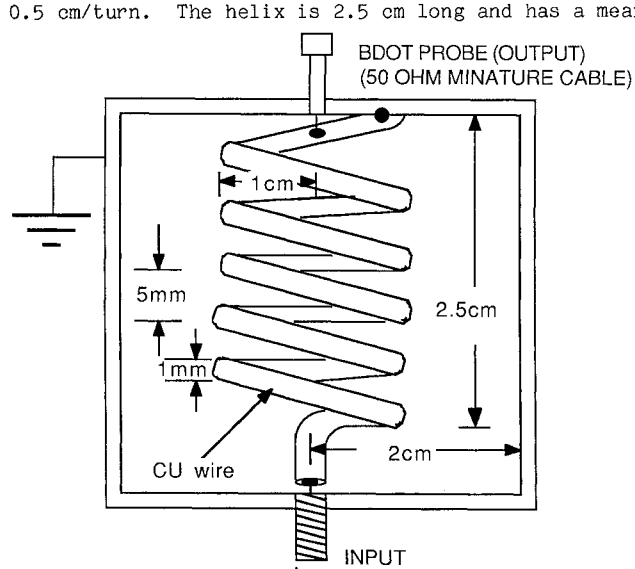

Figure 1. View of 5 turn helix. Input connector is at bottom. 50 Ohm tap-off is at top. Helix is grounded at top.

* Work performed under the auspices of the U.S. Department of Energy by the Lawrence Livermore National Laboratory under contract number W-7405-ENG-48.

Report Documentation Page

Form Approved
OMB No. 0704-0188

1. REPORT DATE	2. REPORT TYPE	3. DATES COVERED
JUN 1987	**N/A**	**-**

4. TITLE AND SUBTITLE
Response Of Helical Structures To High Speed Pulses Or When Can A Helix Be Called An Inductor

5a. CONTRACT NUMBER
5b. GRANT NUMBER
5c. PROGRAM ELEMENT NUMBER

6. AUTHOR(S)

5d. PROJECT NUMBER
5e. TASK NUMBER
5f. WORK UNIT NUMBER

7. PERFORMING ORGANIZATION NAME(S) AND ADDRESS(ES)
Lawrence Livermore National Laboratory Livermore, California 94550

8. PERFORMING ORGANIZATION REPORT NUMBER

9. SPONSORING/MONITORING AGENCY NAME(S) AND ADDRESS(ES)

10. SPONSOR/MONITOR'S ACRONYM(S)
11. SPONSOR/MONITOR'S REPORT NUMBER(S)

12. DISTRIBUTION/AVAILABILITY STATEMENT
Approved for public release, distribution unlimited

13. SUPPLEMENTARY NOTES
See also ADM002371. 2013 IEEE Pulsed Power Conference, Digest of Technical Papers 1976-2013, and Abstracts of the 2013 IEEE International Conference on Plasma Science. Held in San Francisco, CA on 16-21 June 2013. U.S. Government or Federal Purpose Rights License

14. ABSTRACT
Vacuum and dielectric cored loosely wound helices are widely used in pulse power systems. In one extreme, when the applied pulse length is shorter then the transit time in the helix, helices are used as transit time isolators, to lead signals from high voltage terminals to ground [1]. In the other extreme, for pulse durations that are much longer than the transit time, helices act as conventional inductors and are used for high frequency isolation or as shields for trigger, signal or gas leads to pulse power components. In either case, the use of helices in the presence of fast pulses requires an understanding of their behavior in regimes where time delays associated with wave propagation in the helix are not negligible when compared to the length or risetime of the applied pulse and hence their description as lumped elements is no longer correct. This paper describes the results of analytical approximations, circuit simulations, 3-D time dependent electromagnetic modeling as well as laboratory measurements on helices surrounded by conducting structures. On the basis of these investigations their suitability as voltage measuring devices will be discussed.

15. SUBJECT TERMS

16. SECURITY CLASSIFICATION OF:			17. LIMITATION OF ABSTRACT	18. NUMBER OF PAGES	19a. NAME OF RESPONSIBLE PERSON
a. REPORT	b. ABSTRACT	c. THIS PAGE			
unclassified	**unclassified**	**unclassified**	**SAR**	**5**	

diameter of 2 cm so that any "long solenoid" approximations are invalid. A 4 cm-diameter grounded can encloses the helix with one end of the helix attached to the can (in effect, grounding the end of the helix). The beginning of the helix attaches, through a short piece of wire, to a connector embedded in the bottom of the can. This connector is the input port to the helix.

We tapped the uppermost quarter turn of the inductor with a 50 ohm cable, providing an output port to the helix. This connection, acting in effect as a B-dot probe, detects a signal proportional to the derivative of the current that flows to ground in the final turn of the helix.

To develop a circuit model for the helix requires some assumptions about how the energy is distributed in the electromagnetic fields of the helix [8]. It appears reasonable that if the transit time in one turn of the helix is short compared to the risetime of the pulse, the magnetic energy stored in the turn may be represented by the self inductance L_o of the turn. This approximation, of course, assumes that the current is the same throughout the turn. The electric field energy stored between each turn and ground may be represented by the turn-to-ground capacitance C_ℓ. As with the assumption of constant current in the inductor, the assumption is that the voltage is uniform throughout the turn. To account for the electrostatic energy stored between turns we introduce the turn-to-turn capacitance C_t, and, to take into account the magnetic energy due to coupling between turns, we introduce the mutual inductances M_{ij}.

The schematic for a typical single-turn subcircuit appears in Fig. 2. The equivalent circuit model for the five turn helix is comprised of five identical subcircuits, representing the five individual turns of the helix.

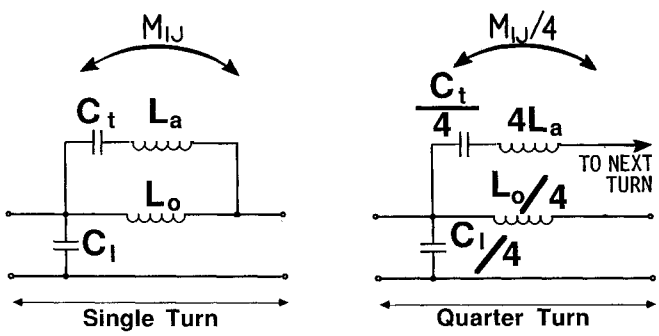

Figure 2. Schematic of single-turn and quarter-turn subcircuits. L_o = 38.6 nH is the single turn inductance, C_ℓ = 0.95 pF is the turn-to-ground capacitance and C_t = 0.76 pF is the turn-to-turn capacitance. L_a = 0.37 nH accounts for the axial turn-to-turn transit time.

The self-inductance L_o for an individual turn assumes a single filamentary current loop. We use Neumann's form [9] with the approximation that d/2R is very small (where d is the diameter of the wire and R is the radius of the loop). This formula assumes that all the current flows in the surface of the wire, and assumes that the return circuit is at infinity. In our case there are no magnetic fields outside the shield so their contributions to the inductance should be zero. Since most of the contribution to the inductance is due to fields in the vicinity of the loop, elimination of the far fields should not appreciably reduce the inductance of each turn. The inductance for each turn is:

$$L_o = \mu_o R\left[\ell n\left(\frac{16R}{d}\right) - 2\right] \text{ [H/turn]} \quad (3)$$

We obtain the turn-to-ground capacitance C_ℓ with the general formula for the capacitance of a single wire near ground [10] with the assumption that $d \ll h$ (where $h = (R_s - R)$ is the height above ground, R_s is the shield radius, c is the speed of light in vacuum, and $\varepsilon = 1$ for air):

$$C_\ell = \left[\left(\frac{60c}{\varepsilon^{1/2}}\right) \ell n\left(\frac{4(R_s - R)}{d}\right)\right]^{-1} (2\pi R) \text{ [F/turn]} \quad (4)$$

We could also have derived the inductance per turn by emphasizing the flux in the area between the turn and the ground plane. In this case the inductance can be easily derived from Eq. 4 as:

$$L_o = N_o R \ell n \frac{4(R_s - R)}{d} \quad (5)$$

For our geometry, the value calculated with this equation is 20% more than the value calculated from Eq. 3. While there is no clear reason to choose expressions (3) or (5), we chose to use (3) because we would be calculating mutual inductances between turns as well.

The turn-to-turn capacitance C_t is calculated using the equation for a two-wire transmission line in air [10] (where s is the wire separation):

$$C_t = \left[(120c)\cosh^{-1}\left(\frac{s}{d}\right)\right]^{-1} (2\pi R) \text{ [F/turn]} \quad (6)$$

In expressions (4) and (6), the term $2\pi R$ accounts for the length of the loop.

An additional inductance L_a appears in series with the turn-to-turn capacitance C_t to provide the circuit branch with the correct time delay (where s is the turn separation):

$$L_a = \left(\frac{s}{c}\right)^2 \frac{1}{C_t} \text{ [H/turn]} \quad (7)$$

The mutual inductances between turns are calculated with the equation for the mutual inductance of coaxial filamentary loops [9] (where K(k) and E(k) are elliptic integrals of the first and second kind, respectively):

$$M_{ij} = \mu_o R\left[\left(\frac{2}{k} - k\right)K(k) - \frac{2}{k}E(k)\right] \text{ [H/turn]} \quad (8)$$

$$k^2 = \frac{4R^2}{4R^2 + s^2} \quad (9)$$

$$K(k) = \int_o^{\pi/2} \frac{d\phi}{\sqrt{1 - k^2\sin^2\phi}} \quad (10)$$

$$E(k) = \int_o^{\pi/2} \sqrt{(1 - k^2\sin^2\phi)}\, d\phi \quad (11)$$

The mutual inductance is found to be 11.3 nH for adjacent turns, 5.00 nH for turns separated by one turn, 2.58 nH for turns separated by two turns, and 1.42 nH for turns separated by three turns.

Given the self inductance of each turn and the mutual inductance between turns, the coupling coefficient between the ith and jth turns becomes:

$$\kappa_{ij} = M_{ij}/(L_i L_j)^{1/2} \quad (12)$$

To increase the time resolution of the model we have refined the single-turn subcircuits into the quarter-turn subcircuits that also appear in Fig 2. To simulate the circuit we have used the circuit code NET-2. The following section compares the results of the simulations with the refined model and measurements performed on the helix.

We recognize our choice of equivalent circuit as the equivalent circuit of a transmission line [12] consisting of cascaded shunt C and series L sections with the added features of mutual inductive and capacitive coupling between sections.

Comparison of Experiments and Simulations

We have performed several laboratory experiments on the helical inductor: frequency-domain input impedance measurements, bridge inductance measurements, time-domain reflectometry measurements, and time-domain pulsed measurements. Each experiment has been simulated using the NET-2 circuit code to obtain insight and to perform some detailed comparisons.

Frequency-domain input impedance measurements were obtained with an HP8510 Network Analyzer. The network analyzer data shows an extremely high input impedance at 190 MHz. The frequency-domain NET-2 simulation shows the first resonance (coinciding with high input impedance) at 195 MHz. These results are in good agreement with one another as well as with the 220 MHz resonant frequency for a shielded helix of this geometry. A design chart [11] for quarter wavelength helical resonators yields the latter value.

Measurements with a network analyzer (HP 3577A) in the 100 kHz to 30 MHz frequency range yield an inductance of 310 nH. For comparison, the inductance for the circuit model was obtained by driving the model with a voltage step function, allowing the transients to decay, and calculating the inductance as $L = V_{in}/dI_{in}/dt$. The inductance resulting from the simulation is 327 nH. The measured and calculated values also compare very well to the 295 nH obtained with a formula for the inductance of a shielded helix [11]:

$$L = (984\ n^2D^2\ell)\left[1 - \left(\frac{D}{D_s}\right)^2\right]\ [nH] \qquad (13)$$

where n is the number of turns per meter, D is the coil diameter, D_s is the shield diameter, and ℓ is the coil length. Curiously enough, the approximations used in the derivation of this formula assume that the axial wavelength and the length of the helix are much larger than D_s. Neither of these conditions applies in our case.

Time-domain reflectometry measurements (TDR) were obtained with a Tektronix 7S12 unit. Measurements show a two-way transit time of 2.3 ns corresponding to a resonant frequency of 217 MHz. The NET-2 TDR simulation show a two-way transit time of 2.9 ns (corresponding to a resonant frequency of 172 MHz). The quantitative interpretation of the TDR transit time measurements is somewhat difficult because the peaks of the waveform are not perfectly defined.

For longer time scales, the TDR waveforms decay exponentially as L/R (where R is 50 ohm and L is the total inductance of the coil), an expected behavior of an inductor. The decay time from the measured TDR data gives an inductance of 311 nH. The inductance obtained from the L/R decay of the NET-2 TDR simulations is 326 nH. As with the previous techniques, the comparison between measurement and calculation is quite favorable.

The pulsed time-domain measurements were obtained with a 50 ohm ps pulser that delivers a 600 ps risetime pulse. A 72 pF shunt capacitor to ground increases the risetime of the pulse to 4 ns. The pulse feeds the helix through a 7.2 ns cable (for transit time isolation). The voltage at the input to the helix is monitored using a 79/1 resistive divider connected at the input.

The signal going into the inductor is trace A of Fig. 3, while the B-dot probe output is shown as trace B. The B-dot probe output consists of two frequency components. One corresponds to the derivative of the input voltage and the other is proportional to the voltage itself.

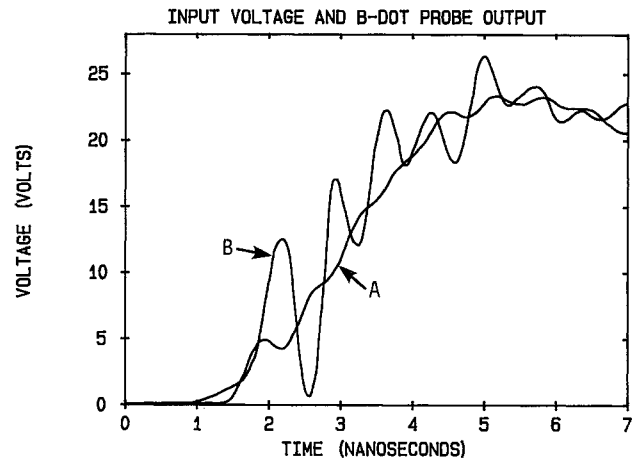

Figure 3. Voltage drive for the helix (A) and B-Dot probe response (B). The B-dot probe response has been scaled by a factor of 27.4.

The input signal into the inductor, as measured by the oscilloscope, was digitized to provide a drive function for the NET-2 model. The NET-2 model's B-dot probe output waveform is compared to the measured output in Fig. 4. The two responses are very similar except for a larger magnitude of the high frequency components in the simulation.

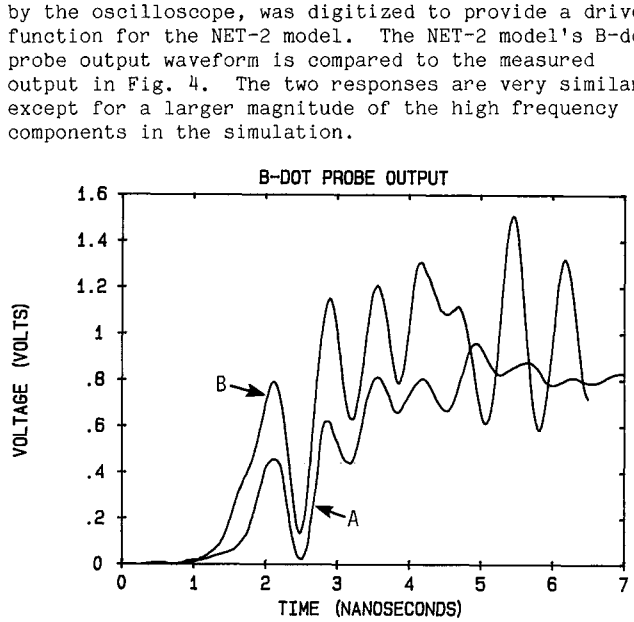

Figure 4. B-dot probe response from the experiment (A) and simulation (B).

Interpretation of Results

The experiments and calculations we have just described provide an excellent vehicle to answer the

question posed in the title of this paper. If we examine the voltage at the input of the helix and the current at the grounded end of the helix, we obtain the incremental current in the helix due to a wave as:

$$\left.\frac{dI}{dV}\right|_{wave} = \frac{2}{Z_o} \quad ; \quad Z_o = \sqrt{L_o/C_\ell} \tag{14}$$

From a circuit standpoint, the incremental current in helix is:

$$\left.\frac{dI}{dt}\right|_{circuit} = \frac{V}{L} \tag{15}$$

If the helix must display inductor-like properties, then:

$$dI|_{wave} \ll dI|_{circuit} \tag{16}$$

and:

$$\frac{1}{V}\frac{dV}{dt} < \frac{1}{2}\frac{Z_o}{L} \tag{17}$$

For our helix, driven by the lumpy voltage waveform displayed in Fig. 3, $1/V\ dV \approx 0.2$, $dt = 0.5$ ns, $Z_o = 200\ \Omega$, and $L_o = 330$ nH violate the conditions of Eq. 17. Hence, the oscillations in the output waveform, are a direct consequence of the transmission line-like behavior of the helix. On the other hand, for our helix driven by the clean voltage waveform displayed in Fig. 5, the conditions of Eq. 17 are not violated. Hence, the output waveform is virtually indistinguishable from the input waveform.

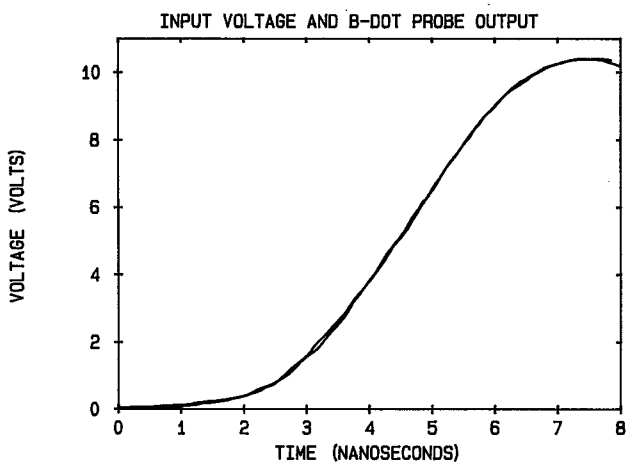

Figure 5. The waveforms for the clean voltage drive for the helix and the B-dot probe response are indistinguishable. The B-dot probe response is scaled by a factor of 27.4.

We therefore conclude that two choices arise in the use of a helix as a voltage monitor. One is to exploit its transmission line properties (pulse duration $\lesssim$ two transit times, current proportional to input voltage). The other choice is to use it as an inductor (pulse duration >> two transit times, current proportional to the integral of the input voltage), subject to the smoothness restrictions on the input voltage waveform imposed by Eq. 17. Note that Eq. 17 is quite general and applies to a loosely wound helix independently of physical size.

ARGUS 3-D Model

We have also performed a simulation of a 3-turn shielded helix with ARGUS [13], a 3-D PIC code, using the E&M solver module only. ARGUS will produce the E and H fields over the whole mesh and will also perform the line integral of E·dl over a path of interest to determine the voltage between two points. We generated turn-to-turn and turn-to-ground voltages with this approach. We also modeled the helix with the circuit techniques described above. The NET-2 and the ARGUS model used a 1.2 mA, 1.2 ns risetime current source.

A comparison of the turn-to-turn voltage for each of the two models (NET-2 and ARGUS) appears in Fig. 6. The two models agree quite well except for a small amount of time shift. This time shift may be due to the fact that the NET-2 [14] model does not include the straight piece of wire at the input whereas the ARGUS model does.

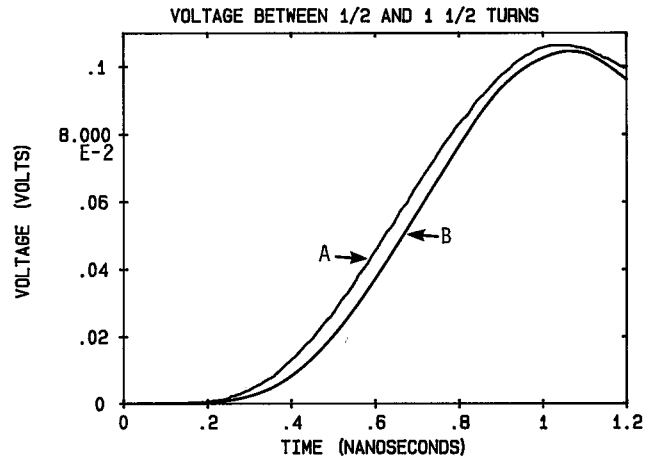

Figure 6. Comparison of turn-to-turn voltages obtained with ARGUS (A) and NET-2 (B).

Examination of the E and H fields in the helix is extraordinarily revealing. Figures 7 and 8 show E and H fields in a mid-section plane of the solenoid containing the centerline and the diameter. At a time when the front of the pulse has just reached the end of the inductor (Fig. 7) shows an E and H distribution that is linear with distance along the helix. This is consistent with a description of the helix as a transmission line driven with a ramp current waveform.

Figure 8 shows the E and H fields in the helix after the reflection from the grounded (bottom) end has reached the feed (top end). The linearly rising current drive produces a constant current distribution in the helix with electric fields that rise linearly with distance along the helix. These are the fields that would be expected for a helical inductor in the quasi-stationary state (constant voltage, linearly rising current).

Conclusions

Our investigations of helical structures have shown that:

(a) These structures behave like transmission lines for short timescales and inductors over longer timescales subject to restrictions on the magnitude of $\dot{V}$ at the input imposed by Eq. 17.
(b) By using simple approximations these structures can be adequately modeled with lumped element networks that account for the energy stored in electric and magnetic fields.
(c) Circuit simulations, 3-D simulations and experimental measurements yield the same physical picture even though fine structure details of the waveforms may vary.

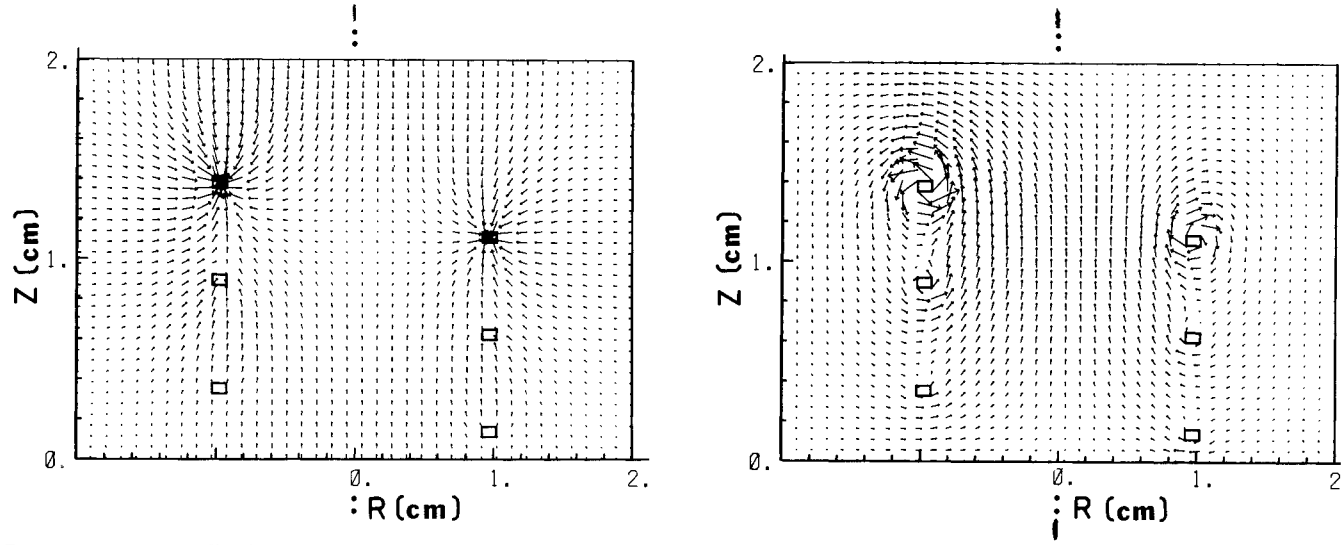

Figure 7. E and H fields for a three turn helix. A current source with a linear rise in time drives the helix at the top. Solenoid is grounded at bottom. Leading edge of pulse has just reached the bottom.

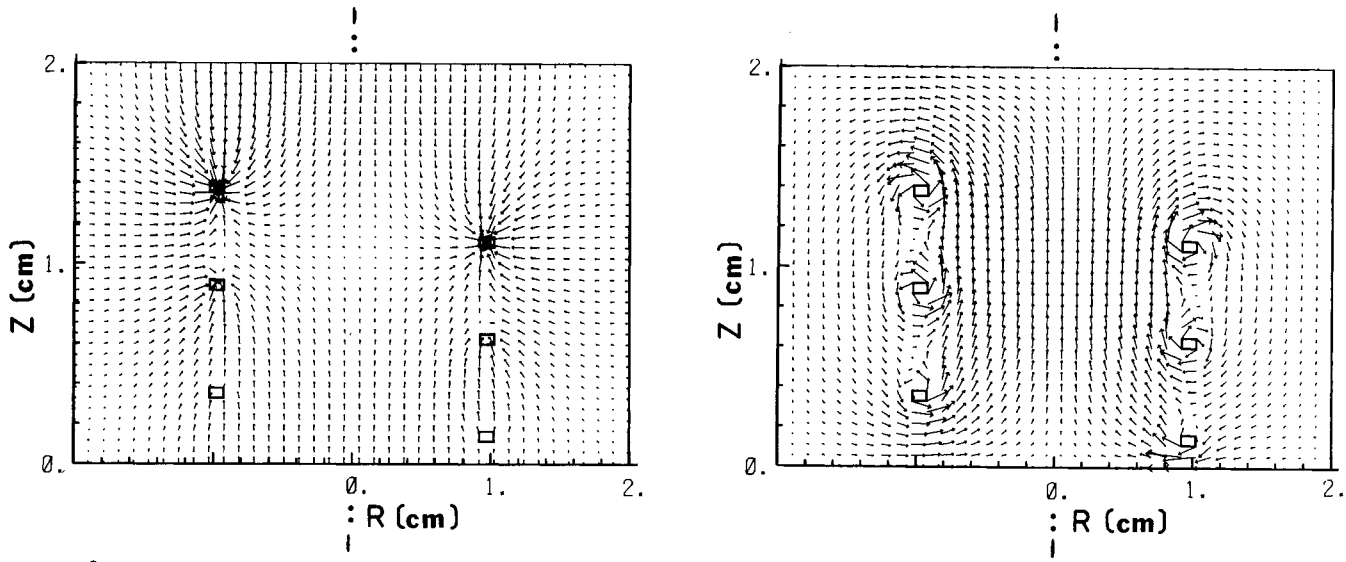

Figure 8. E and H fields for helix. Reflection of pulse from grounded end has just returned to feed end.

References

[1] M. S. Di Capua and D. G. Pellinen, "Magnetic Insulation in Triplate and Coaxial Vacuum Transmission Lines," SAND80-7029, SNLA (1980).

[2] J. R. Carson, "Electromagnetic Theory and the Foundations of Electric Circuit Theory," Bell Sys. Tech. J., 5 , pp. 1-17 (1927).

[3] R. W. P. King, Fundamental Electromagnetic Theory, Dover Pubs., NY, NY (1963).

[4] R. P Feynman, The Feynman Lectures on Physics, Addison-Wesley, Reading, MA (1964).

[5] F. Ollendorf, Die Grundlagen der Hochfrequenztechnik, J. Springer, Berlin (1926).

[6] W. Lenz, "Calculation of Resonant Frequencies of Single Layer Coils," Ann. d. Phys., 43, pp. 749-97 (1914).

[7] A. J Palermo, "Distributed Capacity of Single Layer Coils," Proc. IRE, 22, pp. 897-905 (1934).

[8] J. R. Whinnery, "A Approach to the Solution of High-Frequency Field Problems, Proc. IRE, pp. 284-88 (1944).

[9] S. Ramo, J. R. Whinnery, T. Van Duzer, Fields and Waves in Communication Electronics, 2nd Ed., J. Wiley and Sons, pp. 189-190 (1984).

[10] Reference Data for Radio Engineers, Howard Sams & Co., p. 24-22 (1979).

[11] W. W. McAlpine and R.O. Schildknecht, "Coaxial Resonators with Helical Inner Conductors," Proc. IRE, 47, pp. 2101-2103 (1959).

[12] G. H. Glasoe and J. V. Lebacqz, eds. Pulse Generators, McGraw Hill, NY, pp. 179 and ff. (1948).

[13] ARGUS is a general purpose 3-D plasma simulation code owned by SAIC, McLean VA 22102. Dr. Larry Seftor constructed the input deck.

[14] A. Malmberg, "NET-2 Network Analysis Program," HDL-050-01, Harry Diamond Laboratories DAAG 39-77-C-0050 and 150 (1977).